

MEASUREMENTS OF  $(\vec{p}, \vec{p}')$  AND  $(\vec{p}, p'\gamma)$  OBSERVABLES  
FOR  $1^+$  STATES IN  $^{12}\text{C}$  AT 200 MeV

S.P. Wells, S.W. Wissink, A.D. Bacher, G.P.A. Berg, S.M. Bowyer,  
S. Chang, W. Franklin, J. Liu, and E.J. Stephenson  
*Indiana University Cyclotron Facility, Bloomington, Indiana 47408*

J. Beene, F. Bertrand, M. Halbert, P. Mueller, D. Olive, and R. Varner  
*Oak Ridge National Laboratory, Oak Ridge, Tennessee 37831*

J. Lisantti  
*Centenary College of Louisiana, Shreveport, Louisiana 71134*

K. Hicks  
*Ohio University, Athens, Ohio 45701*

The study of  $(\vec{p}, \vec{p}')$  spin observables has historically provided valuable information about the NN interaction inside the nuclear medium.<sup>1</sup> There are, however, only eight independent quantities that can be determined in singles  $(\vec{p}, \vec{p}')$  reactions. For transitions to discrete states of non-zero spin  $J$ , additional information can be obtained by studying the polarization of the recoil nucleus. This is possible through measurements of the angular correlation between the scattered proton and the particles emitted in the nuclear de-excitation. For transitions with the simple spin sequence  $0^+ \rightarrow 1^+$ , measurements of the type  $(\vec{p}, p'\gamma)$ , in which the polarizations of the outgoing proton and photon are not detected, when combined with the complete sets of  $(\vec{p}, \vec{p}')$  observables discussed above, provide sufficient information to completely specify the scattering amplitude.<sup>2</sup> Using the K600 spectrometer and its associated focal plane polarimeter (FPP) to detect the scattered protons, and a system of  $\text{BaF}_2$  detectors<sup>3</sup> surrounding the K600 target to detect the coincident  $\gamma$ -rays, we have performed simultaneous measurements of  $(\vec{p}, \vec{p}')$  spin-transfer observables as well as  $(\vec{p}, p'\gamma)$  coincident observables for the two dominant  $1^+$  states in  $^{12}\text{C}$  ( $T=1$  at 15.11 MeV,  $T=0$  at 12.71 MeV) at a proton bombarding energy of 200 MeV.

Because  $(\vec{p}, \vec{p}')$  measurements provide at most eight pieces of information, yet eleven are required for a complete determination of the scattering amplitude (for  $0^+ \rightarrow 1^+$  transitions), it can be shown<sup>2</sup> that  $(\vec{p}, p'\gamma)$  observables contain information about the transition which is not accessible in  $(\vec{p}, \vec{p}')$  singles measurements. The full scattering amplitude can be divided into two parts: terms involving the proton spin coupled to unit vectors in the reaction plane, and terms where the proton spin couples to the unit vector normal to the scattering plane. It is the relative phases between these two sets of terms that can be measured via  $(\vec{p}, p'\gamma)$  observables and are not accessible in  $(\vec{p}, \vec{p}')$  measurements. It can also be shown<sup>2</sup> that if the coincident  $\gamma$ -rays are detected at some angle out of the reaction plane, yet not normal to it, then the photon polarization tensor will have negative parity. In this case, the sideways and longitudinal analyzing powers,  $D_{0S}$  and  $D_{0L}$ , which are identically zero in singles  $(\vec{p}, \vec{p}')$  measurements due to parity conservation, may be non-zero. Contained in these asymmetries are the relative phases just discussed. By placing three of the  $\text{BaF}_2$  arrays at an angle of  $45^\circ$  out of the scattering plane, we were able to map out the angular distribution of these previously unmeasured asymmetries.

Because  $0^+ \rightarrow 1^+$  transitions are of unnatural parity, they are dominated by an orbital angular momentum change of  $\Delta L = 0$ . As such, the differential cross sections for exciting these states are very forward peaked in the laboratory frame. To obtain appreciable yields for these studies, it was therefore necessary to place the entrance to the K600 spectrometer at small laboratory scattering angles. Moreover, since the BaF<sub>2</sub> detectors were positioned very near the target chamber, it was necessary to deposit the unscattered beam in a well-shielded beam dump far downstream from the target. To meet both of these requirements, we utilized the septum magnet mode of the K600 spectrometer.<sup>4</sup> In this mode, we were able to detect cleanly coincident  $\gamma$ -rays associated with protons scattered at laboratory angles as small as  $\theta_p = 5^\circ$ . In order to minimize the attenuation of the coincident  $\gamma$ -ray flux and to ensure that this attenuation was independent of  $\theta_\gamma$ , a special thin-walled scattering chamber compatible with all septum magnet mode hardware was installed for these measurements. This scattering chamber was cylindrical in shape, with the symmetry axis perpendicular to the scattering plane. The aluminum chamber had 0.25" thick walls and an outer diameter of 10". A 0.25" thick upper lid was also used since, for reasons discussed below, one BaF<sub>2</sub> array was placed directly above the target to detect coincident photons emitted along the normal to the scattering plane. With this choice of geometry for the scattering chamber, and given the positioning of the BaF<sub>2</sub> arrays (discussed below), the attenuation of the emitted  $\gamma$ -ray flux was independent of photon angle and approximately 4% for  $E_\gamma = 15$  MeV.

In April 1993, we were given 28 shifts of beam to carry out measurements of  $(\vec{p}, \vec{p}')$  singles spin observables and  $(\vec{p}, p'\gamma)$  coincident observables for the  $1^+$  states in <sup>12</sup>C at 200 MeV. Measurements were made with the BaF<sub>2</sub> arrays in two different configurations. In the first configuration, using an incident proton beam polarized normal to the scattering plane, three BaF<sub>2</sub> arrays were positioned on beam right lying in the scattering plane at angles of  $\theta_\gamma = 60^\circ, 100^\circ,$  and  $140^\circ$  with the front face of each array at a distance of 56 cm from the target. Due to the large charged-particle flux emitted at forward angles from the 93.8 mg/cm<sup>2</sup> <sup>NAT</sup>C target, it was necessary to place 3.6 cm of aluminum in front of the BaF<sub>2</sub> array at  $\theta_\gamma = 60^\circ$ , which was sufficient to stop protons of  $\sim 100$  MeV. In this configuration, we made measurements of the singles observables  $d\sigma/d\Omega$ ,  $A_y$ ,  $P$ , and  $D_{NN'}$ , and simultaneously measured the coincident cross section  $d^2\sigma/d\Omega_\gamma d\Omega_p(\vec{k})$  and coincident asymmetry  $A_y(\vec{k})$  as a function of photon angle in the scattering plane. (Here  $\vec{k}$  is the momentum of the emitted photon.) Using the BaF<sub>2</sub> array placed directly above the target, we also measured the coincident cross section and asymmetry, both of which can be related,<sup>2</sup> in a model independent way, to the singles spin-transfer observable  $D_{NN'}$ . Since we were simultaneously measuring this observable in the FPP, we thus obtained a valuable internal consistency check on the data. Measurements were made at proton scattering angles of  $\theta_p = 5^\circ, 8^\circ, 11^\circ,$  and  $15^\circ$ . Shown in Fig. 1 is a schematic diagram of the configuration used for these measurements. Walls of lead were stacked both upstream and downstream of the BaF<sub>2</sub> detectors to shield from  $\gamma$ -rays emitted from beam-line elements and the external beam dump, respectively.

In the second configuration, where we used an incident proton beam which had its polarization vector rotated *into* the scattering plane, we supported three BaF<sub>2</sub> arrays at an angle of  $45^\circ$  out of the scattering plane. In this case, the BaF<sub>2</sub> arrays were positioned

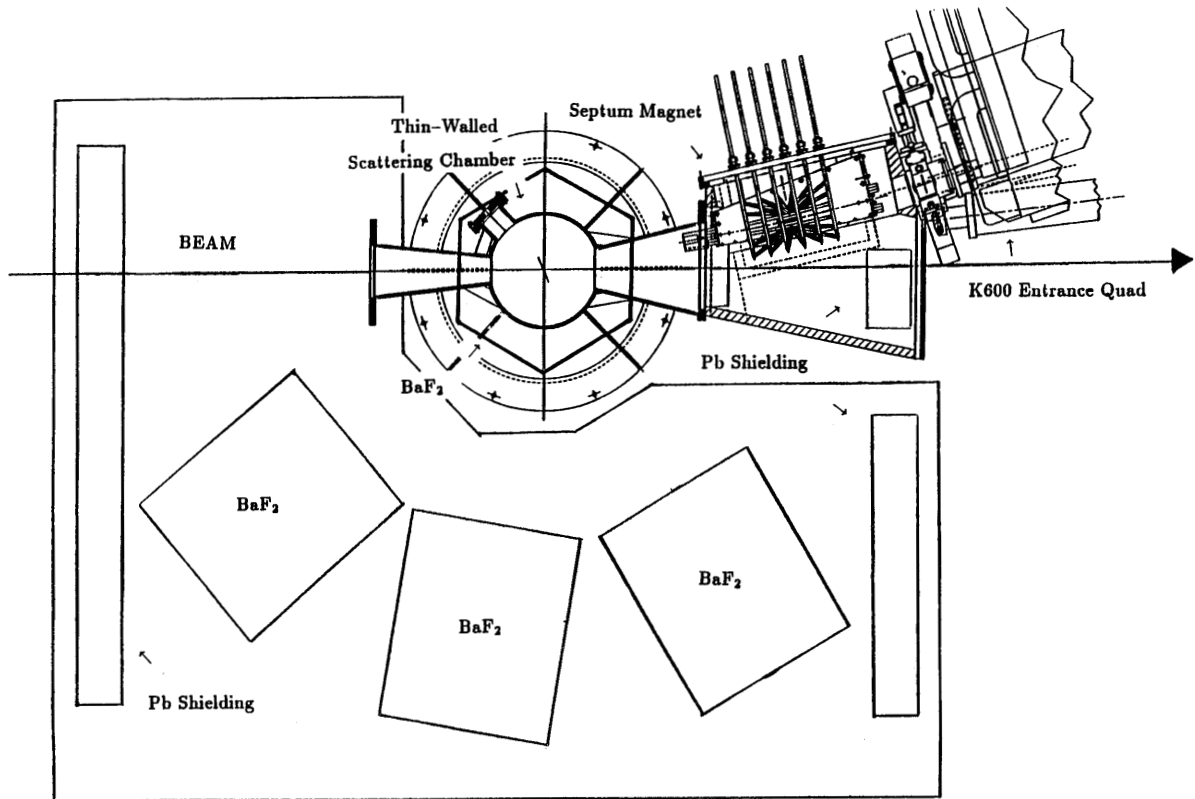
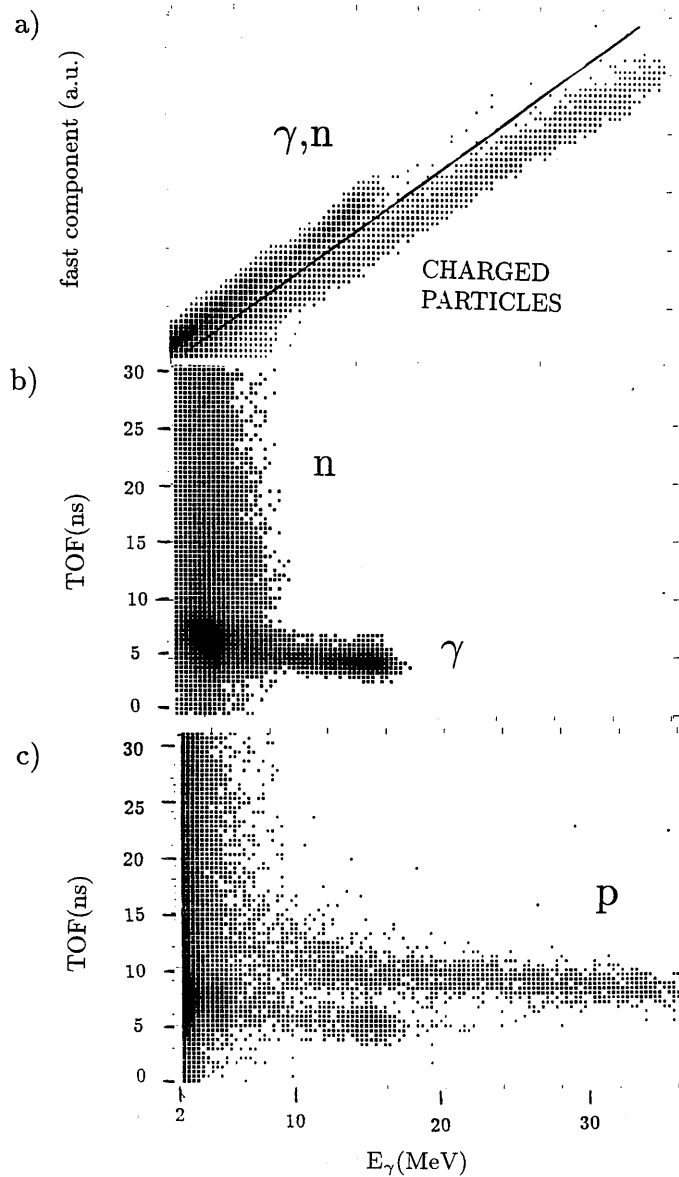


Figure 1. Schematic diagram showing the position of the four  $\text{BaF}_2$  arrays relative to the thin-walled scattering chamber, septum magnet hardware, and K600 entrance quadrupole. Distances and angles of the arrays are given in the text. Walls of lead were stacked both upstream and downstream of the arrays to shield them from radiation generated from beamline elements and the beam dump, respectively.

on beam right at angles of  $\theta_\gamma = 41^\circ, 88.3^\circ,$  and  $140^\circ$ . Due to space limitations, we were forced to place the centers of the arrays at distances of 79 cm, 66 cm, and 66 cm from the target, respectively. In this configuration, we measured two linear combinations of the four singles spin-transfer coefficients  $D_{LL'}$ ,  $D_{LS'}$ ,  $D_{SL'}$ , and  $D_{SS'}$  as well as the induced polarization  $P$  (which is independent of the incident beam polarization) in the FPP. The  $\text{BaF}_2$  arrays were used to map out an angular distribution of the photon yield asymmetries for the measurement of the sideways and longitudinal analyzing powers  $D_{0S}$  and  $D_{0L}$ . In order to separate the sideways and longitudinal pieces, it is necessary to have at least two orientations of the incident proton spin in the scattering plane. To provide internal consistency in these measurements, we chose to make measurements with the incident proton polarization in three different orientations, at in-plane angles of  $\Phi = 53^\circ, 117^\circ,$  and  $169^\circ$  with respect to the incident beam direction. Again, data were taken at proton scattering angles in the lab of  $\theta_p = 5^\circ, 8^\circ, 11^\circ,$  and  $15^\circ$ .

In our experiment, three signals were read out by CAMAC for each photon detector that satisfied a low threshold discriminator in hardware coincidence with the detection of a proton in the K600 focal plane: fast timing information, relative to the K600 focal plane scintillators; a wide-gate integrated pulse height, for good photon energy resolution over the energy range of primary interest; and a short-gate pulse height, the amplitude of which is dominated by the fast (ultraviolet) component of the scintillator response.<sup>4</sup> These three signals provide sufficient information to cleanly separate pulses generated by photons from those generated by fast neutrons and charged particles.<sup>5</sup> These latter types of particles can be identified by exploiting the lower relative intensity of the fast component that these types of particles generate. Figure 2a shows the correlation between the fast component and the total light output for all coincident events in the BaF<sub>2</sub> array positioned at  $\theta_\gamma = 100^\circ$ . Charged and neutral particles are located in two distinct bands in this correlation. Shown in Fig. 2b and 2c are the correlations between the total light output (the wide-gate integrated pulse height) and the relative p- $\gamma$  time-of-flight difference for the two distinct bands shown in Fig. 2a. Because at  $\theta_p = 8^\circ$  the yields for the 4.44 MeV and 15.11 MeV states dominate the proton energy spectrum (with the p+<sup>12</sup>C elastic peak vetoed in hardware), one expects an enhancement of the coincident photon yield at these two energies. This is clearly shown in Fig. 2b where, at the shortest relative time-of-flight, two maxima are visible at photon energies of 4.44 and 15.11 MeV. There is also some fraction of coincident photons which generate pulses of identical shape as those produced by charged particles (the origin of these events is still under investigation). With the time-of-flight vs. energy correlation, however, these events can be separated from charged particles, as shown in Fig. 2c. While this preliminary offline analysis indicates that ( $\vec{p}, p'\gamma$ ) events from the 15.11 MeV, 1<sup>+</sup> state in <sup>12</sup>C can be easily identified, further analysis (such as accidental beam-burst subtraction) is required to extract any coincident ( $\vec{p}, p'\gamma$ ) observables.

1. See, for example, H. Bagheai, *et al.*, Phys. Rev. Let. **69**, 2054 (1992), and references therein.
2. J. Piekarewicz, *et al.*, Phys. Rev. C **41**, 2277 (1990).
3. M. Thoennessen, J.R. Beene, F.E. Bertrand, and J.L. Blankenship, Oak Ridge Nat. Lab. Prog. Rep. (1989).
4. G.P.A. Berg, *et al.*, this report.
5. R. Novotny, *et al.*, Nucl. Instrum. Methods A **262**, 340 (1987).



*Figure 2.* (a) Intensity distribution of the fast light component versus the total light output of all BaF<sub>2</sub> crystals in the 19-pack placed at  $\theta_\gamma = 100^\circ$ . Requirements for incrementing this histogram are given in the text. Charged particles are discriminated from photons and neutrons as indicated by the solid line. (b) Intensity distribution of the relative time-of-flight versus total  $\gamma$ -ray energy for photons and neutrons as identified in (a) (above the solid line). (c) Same as (b) for charged particles and photons (below the solid line).